International Journal of Organizational Innovation

THE MAJOR CAUSE FOR THE DESTRUCTION OF THE GANGWEIGOU CREEK FLOODWAY

Tse-Shan Hsu
President, Institute of Mitigation for Earthquake Shear Banding Disasters
Professor, Department of Civil Engineering, Feng-Chia University
Taiwan, R.O.C.
tshsu@fcu.edu.tw

Ming-Tuo Chen
Ph.D. Program for Civil Engineering, Water Resources Engineering, and Infrastructure Planning, Feng-Chia University, Taiwan, R.O.C.

Shey-En Chiu
Water Resources Agency, Ministry of Economic Affairs
Taiwan, R.O.C.

Abstract

At present, all hydraulic structure design codes have not fortified the main effect of tectonic earthquakes. Therefore, although the designs provided by the technicians have fully met the requirements of the code, the hydraulic structures after completion will still have localized piping failure problems under shear banding effect. In view of this, the authors of this paper have conducted an in-depth study of the piping failure induced landslides in Gangweigou River Floodway in Tainan, Taiwan. The results of the study reveal that because the piping failure mechanism proposed by Terzaghi is based on the steady-state groundwater seepage flow with mass conservation, after it was adopted by the technicians, most of them were unable to obtain results consistent with actual piping failures; and actual piping failures only occur locally in the shear bands, where the degree of brittle fracture of the soil stratum increases with the increase in the amount of shear banding, so soil particles will flow out along the pipelines formed by the pore space in the shear band. Therefore, the condition of initiating piping failure is redefined as the bottom velocity of particles in the shear band being greater than or equal to the critical bottom velocity of the particles. Finally, it is suggested that the shear banding effect and the new piping failure mechanism proposed by the authors should be incorporated into the hydraulic structure design specifications, so as to ensure that the design provided by the technician is safe and the major cause of the disasters provided by the investigator is correct in the future. The results of the study reveal the following. (1) Because the piping failure mechanism proposed by Terzaghi, the father of soil mechanics, is based on the steady-state groundwater seepage flow with mass conservation, after it was adopted by the technicians, most of them were unable to obtain results consistent with actual piping failures. (2) Piping failures only occur locally in the shear bands, where the degree of brittle fracture of the soil stratum increases with the increase in the amount of shear banding, so soil particles will flow out along the pipelines formed by the pore space in the shear band. Therefore, the condition of initiating piping failure is redefined. Finally, it is suggested that the shear banding effect and the new piping failure mechanism proposed by the authors should be incorporated into the hydraulic structure design specifications, so as to ensure that the design provided by the technician is safe and the major cause of the disasters provided by the investigator is correct in the future.

Keywords: hydraulic structures, shear banding, piping failure, bottom velocity.

Introduction

Although the design of all hydraulic structures in Taiwan must comply with the specifications of the existing design codes, (Water Resources Bureau of Ministry of Economic Affairs, 2003, 2008), and these design codes have continuously revised based on the causes of the collapses of the hydraulic structures obtained from the investigations. However, even the new hydraulic structures will collapse just after completion, and all subsequent investigations into the cause of collapse are based on the same specifications. Therefore, whether the design specifications of hydraulic structures correctly fortify the major cause of the collapses for the hydraulic structures actually affects the accuracy of the design and investigation results.

If the investigated major cause of the collapsed hydraulic structures does not meet the actual needs, the revision of the specifications cannot be correct. Thereafter, similar collapses will occur repeatedly. Thus, in this paper, the authors firstly utilized the piping failure mechanism and piping resistance safety factor proposed by Terzaghi (1943) to conduct a case study for the piping failure of Gangweigou Creek Floodway. The results showed that Terzaghi (1943) utilized the mass-conservation steady-state groundwater seepage flow to construct the mass-non-conservation unsteady-state piping failure mechanism. Thus the analysis results are difficult to meet the actual needs. In order to make the analysis results meet the actual needs, the authors propose a new piping failure mechanism based on the mass-non-conservation unsteady-state groundwater pipe flow, and present a governing equation for the initiation of piping failure. Finally, a case study results are used to prove that the new mechanism and governing equation proposed by the authors can lead the analysis results to meet the actual needs.

Piping Failure Mechanism Proposed by Terzaghi

Terzaghi (1943) adopted a net of seepage flow lines and equipotential lines shown in Figure 1 to propose a piping failure mechanism. When the embedded depth of the sheet pile wall under the excavation surface is D, Terzaghi (1943) proposed that the excavation surface within D/2 range from the sheet pile wall will heave upwards due to piping failure.

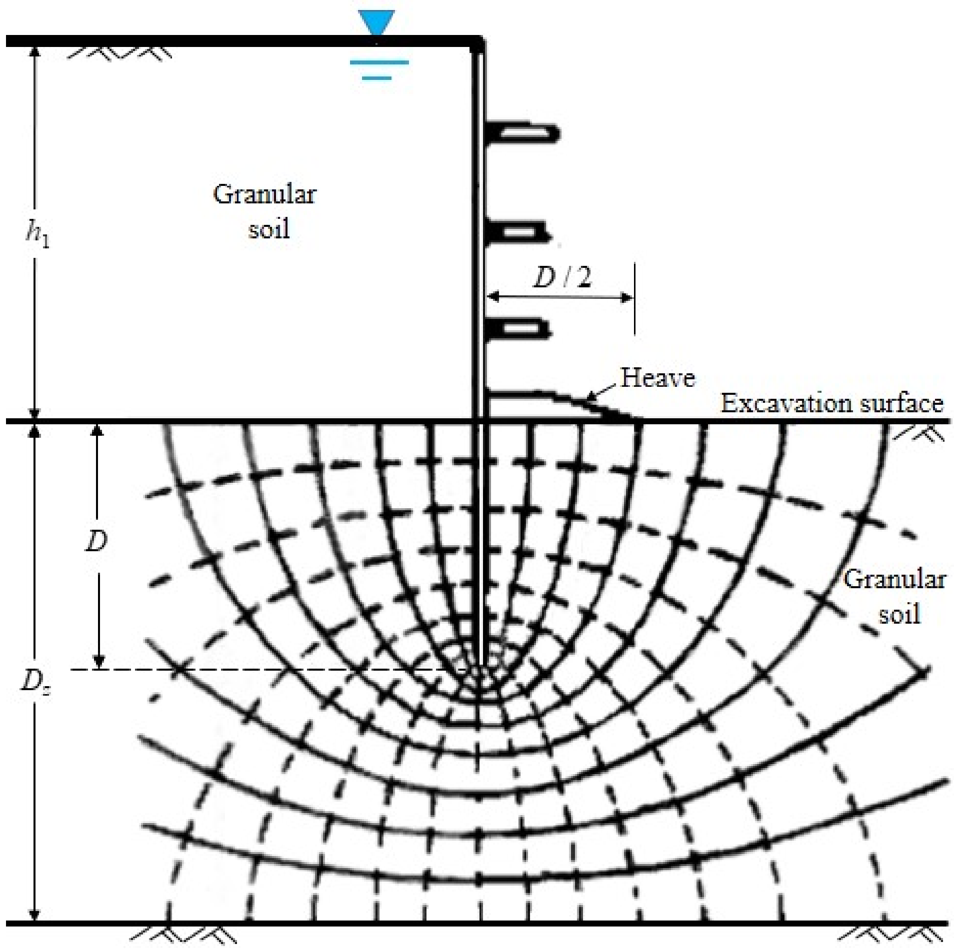

Figure 1. Grid of seepage flow lines and equipotential lines with sheet pile wall as excavation support (modified from Terzaghi, 1943).

When the third direction of the sheet pile wall is long enough, the plane strain conditions can be applied to the soil column shown in Figure 2 in an analysis; thereafter, Terzaghi (1943) defined the safety factor against piping as $FS = W'/U_s$, where W' is the effective weight of the soil column submerged in groundwater, that is, $W' = (\gamma_{sat} - \gamma_w)D^2/2$; and U_s is the upward buoyancy acting on the bottom of the soil column, and its value can be determined by the average value of water head h_{ave} for the equipotential lines passing through the bottom of the soil column, thus, $U_s = h_{ave}\gamma_w D/2$, and $FS = (\gamma_{sat} - \gamma_w)D/(h_{ave}\gamma_w)$. Therefore Terzaghi (1943) defined that the piping failure will occur when $FS \leq 1.0$.

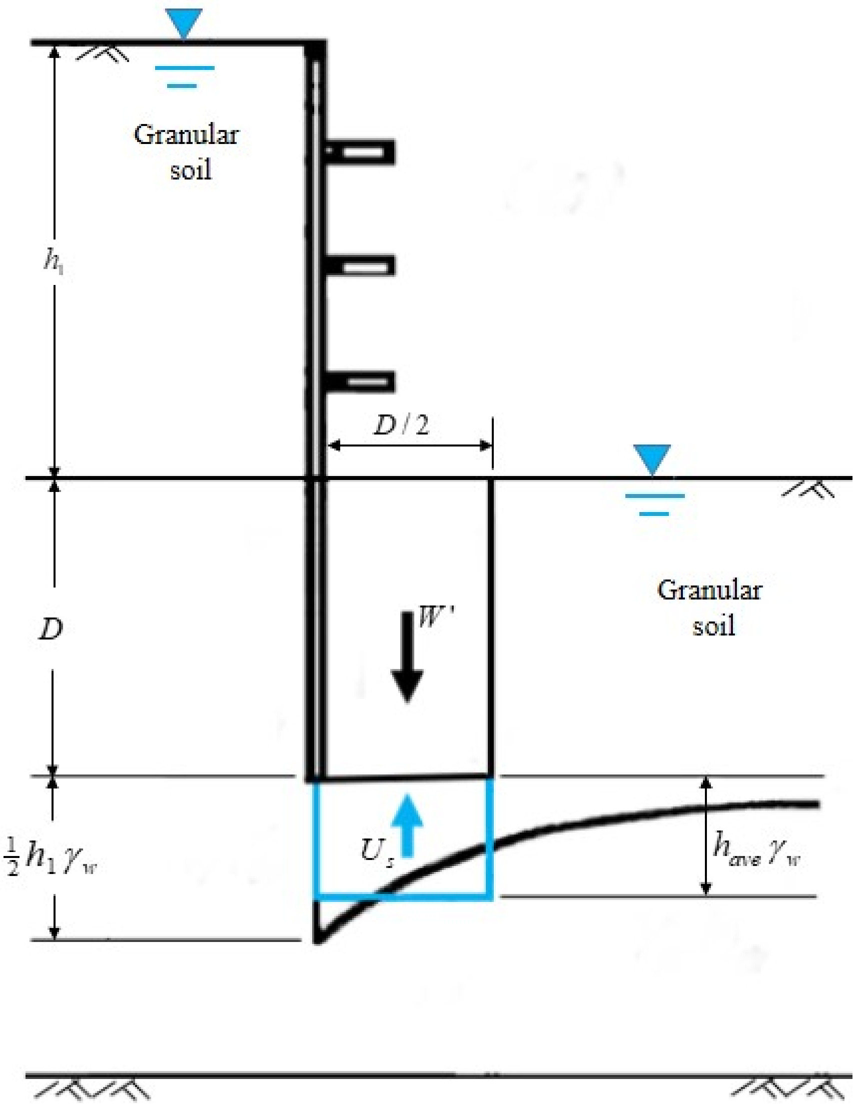

Figure 2. W' and U_s used to determine the safety factor against piping.
(modified from Terzaghi, 1943).

Piping Failure Mechanism Proposed by the Authors

When the sheet pile wall is embedded in a shear band, because of the brittle-fractured effect, the pore space of the shear band will be connected in series to form pipelines, the flow pattern in the shear band will change from seepage flow to pipe flow. In the pipe flow process, the groundwater will entrain soil particles and flow upwards along the pipelines. The soil particles that have flowed out will finally stay on the excavation surface (Figure 3).

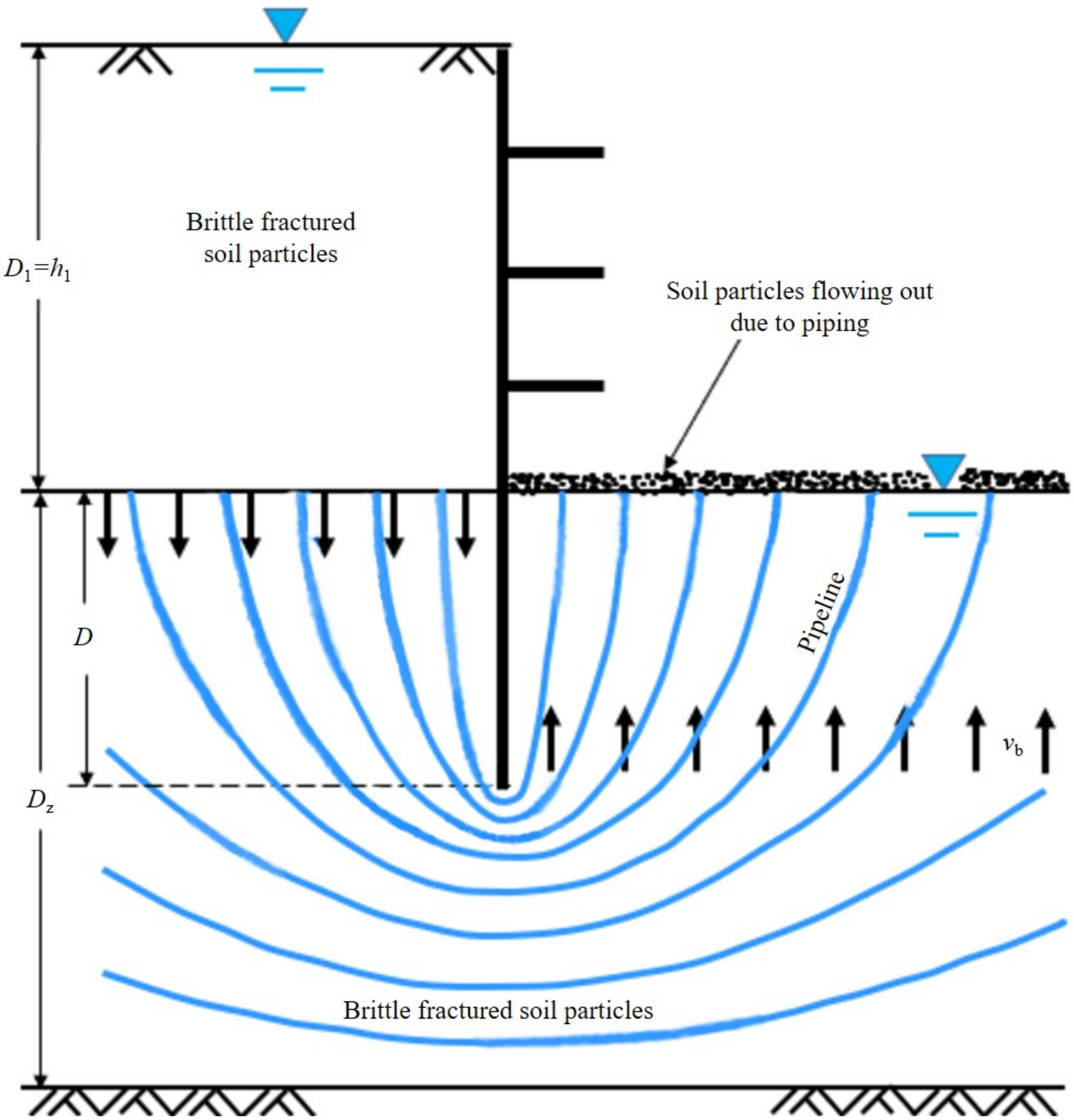

Figure 3. Schematic diagram of pipe flow in a shear band.

Generally speaking, the head loss due to seepage flow is much greater than that of pipe flow. Therefore, the grid of seepage flow lines and equi-potential lines (Figure 1) cannot be used to construct a piping failure mechanism. Thus the pipe flow in the shear band shown in Figure 3 is adopted by the authors to construct a new piping failure mechanism. When the pore spaces of the brittle fractured shear band are connected in series to form a tubular outlet, and the bottom velocity v_b of the soil particles is greater than the critical velocity v_{bc}, the particles will flow with the groundwater after floating, which will cause piping failure. Therefore $v_b > v_{bc}$ is the condition for the initiation of piping failure; and v_{bc} can easily be determined by using Equation 1 proposed by Hsu et al (2014).

$$v_{bc} = \sqrt{\frac{2g(G_s - 1)}{1+e}} \cdot \sqrt{D_p} \cdot \cos\beta \qquad \text{(Equation 1)}$$

Where g is the acceleration of gravity, G_s is the specific gravity, e is the void ratio, D_p is the particle size, and β is the inclination angle of the deposition surface for soil particles.

When g = 9.807 m/s^2, G_s = 2.65, $\beta = 0^\circ$, Equation 1 can be rewritten as:

$$v_{bc} = 5.689 \cdot \sqrt{\frac{D_p}{1+e}} \qquad \text{(Equation 2)}$$

When the brittle-fractured particles in the shear band, from small to large, accompanied by the outflow of groundwater, Table 1 shows that the calculated critical bottom velocity v_{bc} changes with the change of particle size D_p and void ratio e of floating particles.

Table 1. The critical bottom velocity changes with the change of particle size and void ratio of floating particles.

Soil classification	Particle size, D_p	Critical bottom velocity, v_{bc} (m/sec)		
		e = 1.5	e = 2.0	e = 2.5
Silt	0.05 mm	0.025	0.023	0.022
Sand	0.1 mm	0.036	0.033	0.030
Sand	0.5 mm	0.080	0.073	0.068
Sand	1 mm	0.114	0.104	0.096

Gravel	5 mm	0.254	0.232	0.215
Gravel	1 cm	0.360	0.328	0.304
Gravel	5 cm	0.805	0.734	0.680
Cobble	10 cm	1.138	1.039	0.962
Boulder	50 cm	2.544	2.322	2.150

Case Study

Problem description

Figure 4 shows the original drainage system of Baoan Industrial Area, Guiren District, and Rende District of Tainan, Taiwan, which includes Gangweigou Creek, Erren Creek, Zhongzhou Drainage Ditch, etc.

Due to the increasing intensity of heavy rain, the flooding situation in Baoan Industrial Zone and Rende District is becoming more and more serious. In order to reduce the flooding problem in these two areas, the Water Resources Agency of the Ministry of Economic Affairs and the Tainan City Government jointly promoted the plan of Gangweigou Creek Floodway in 2005.

Figure 4 shows that Gangweigou Creek Floodway is located on the east side of National Highway No. 1. It was hoped that after the completion of the plan, the flood of Erren Stream in the Guiren District can directly pass through the Gangweigou Creek Floodway to the Gangweigou Creek in the north. Under this circumstance, the flood will no longer flow westwards into the Rende District and Baoan Industrial Area; thus the design goals of this plan can be achieved.

Generally speaking, the meandering creek shown in Figure 4 clearly indicated that there are displaced landform features; and the displaced landform features originate from shear banding effect. Therefore, the higher the meandering degree of a creek, the more significant the shear banding effect that the creek has suffered in the past history.

Thus, in the process of designing Gangweigou Creek Floodway, it is necessary to consider the influence of the shear banding effect existing in the area surrounded by Erren Creek and Gangweigou Creek. Only in this way can the stability of the hydraulic structure be ensured.

Taking the Gangweigou Creek Floodway as an example, Figure 5 shows the floodway just after it was completed. It is revealed from Figure 5 that there are meandering deep grooves in Gangweigou Creek Floodway, and the shear bands that produces the grooves will extend outward to both sides of the floodway; therefore, when designing the sheet pile wall, the shear banding effect must be taken into account. Otherwise, the sheet pile walls on both sides of the floodway will collapse along with the occurrence of piping failure (Figure 6).

Legend

: Gangweigou Creek
: Gangweigou Creek Floodway
: Erren Creek
: Zhongzhou Drainage Ditch

Figure 4. Geographical map of Gangweigou Creek Floodway (epaper.wra.gov.tw, 2015).

Figure 5. Gangweigou Creek Floodway just after completion (Qi, 2014).

(a) One-step sheet pile wall

(b) Two-step sheet pile wall (Wu, 2016)

Figure 6. Gangweigou Creek Floodway just after the collapse.

Piping failure analyses

1) Adopting the piping failure mechanism proposed by Terzaghi (1943)

(1) One-step sheet pile wall

For the one-step sheet pile wall of Gangweigou Creek Floodway shown in Figure 7, piping failure is likely to occur when the groundwater table of the soil behind the sheet pile wall is 436 cm above the creek bed (i.e. $h_1 = 4.36$ m), the specific gravity of soil G_s is 2.65, the void ratio e is 1.5, the unit weight of soil after submerged in the groundwater γ_{sub} is 6.47kN/m^3, the embedding depth of sheet piles D is 7.64 m, and h_{ave} shown in Figure 2 is 1.64 m. Then the calculated safety factor of piping resistance FS by using the formula proposed by Terzaghi (1943) is 3.07. Such a result indicates that the piping failure will not occur in the soil behind the one-step sheet pile wall.

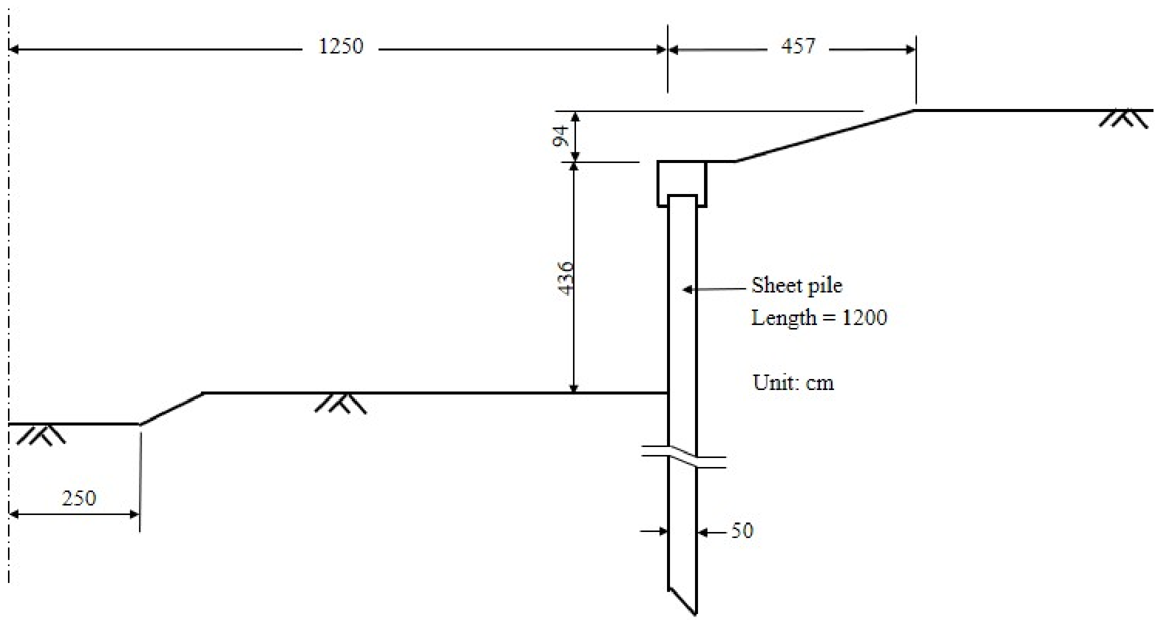

Figure 7. One-step sheet pile wall (epaper.wra.gov.tw, 2015).

(2) Two-step sheet pile wall

For the two-step sheet pile wall of Gangweigou Creek Floodway shown in Figure 8, piping failure is most likely to occur at the upper-step sheet pile wall when the groundwater table of the soil behind the upper-step sheet pile wall is 400 cm above the upper-step creek bed (i.e. $h_1 = 4$ m), the specific gravity of soil G_s is 2.65, the void ratio e is 1.5, and the unit weight of soil after submerged in the groundwater γ_{sub} is 6.47 kN/m^3, the embedding depth of sheet piles D is 8 m, and h_{ave} shown in Figure 2 is 1.5 m. Then the safety factor of piping resistance FS calculated by using the formula proposed by Terzaghi (1943) is 3.52. Such a result also indicates that the piping failure will not occur in the soil behind the two-step sheet pile wall.

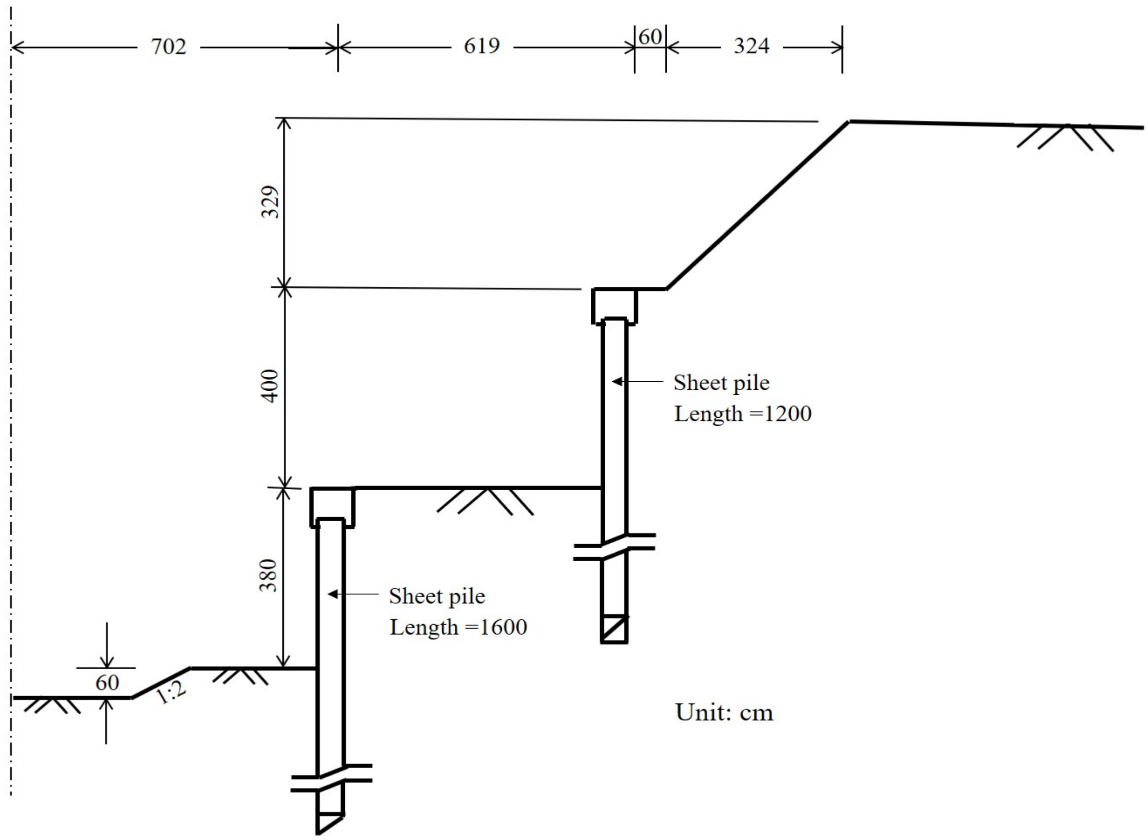

Figure 8. Two-step sheet pile wall epaper.wra.gov.tw, 2015).

2) Adopting the piping failure mechanism proposed by the authors

(1) One-step sheet pile wall

For the one-step sheet pile wall of Gangweigou Creek Floodway shown in Figure 7, the piping failure is likely to occur when the groundwater table of the soil behind the sheet pile wall is 436 cm above the creek bed (i.e. $h_1 = 4.36$ m), the soil specific gravity G_s is 2.65, the void ratio e is 1.5, and the inclination angle of the brittle-fractured soil deposition surface in the shear zone β is 0°. If the pore space of the shear band will be connected in series to form pipelines, and the efficiency coefficient E of the flow velocity of water in the tubular outlet is only 1%, the calculated particle bottom velocity $v_b = E\sqrt{2gh_1} = 0.092\,m/s$. Under the above conditions, it is known from Table 1 that the bottom velocity v_b is greater than the critical bottom velocity v_{bc} for the brittle-fractured particles with particle sizes $D_p \le 0.5\,mm$; so there is a slight piping failure problem.

When particles with their sizes $D_p \le 0.5\,mm$ have flowed out, the void ratio e increases from 1.5 to 2.0, and the efficiency coefficient E increases from 1% to 5%, the calculated particle bottom velocity v_b is equal to 0.46 m/s. Under the above conditions, it is known from Table 1 that the bottom velocity v_b is greater than the critical bottom velocity v_{bc} for the brittle-fractured particles with a particle sizes $D_p \leq 1$cm; so there is a significant problem of piping failure.

When the particles with their sizes $D_p \leq 1$ cm have flowed out, the void ratio e increases from 2.0 to 2.5 and the efficiency coefficient E increases from 5% to 10%, the calculated particle bottom velocity $v_b = 0.92 m/s$. Under the above conditions, it is known from Table 1 that the bottom velocity v_b for the brittle-fractured particles with a particle size $D_p \leq$ 5 cm is greater than the critical bottom velocity v_{bc}; so there is a very significant problem of piping failure.

(2) Two-step sheet pile wall

For the two-step sheet pile wall of Gangweigou Creek Floodway, as shown in Figure 8, the piping failure is most likely to occur when the groundwater table of the soil behind the sheet pile wall is 400 cm above the upper creek bed of Gangweigou Creek Floodway (i.e. h_1 = 4 m), the specific gravity of soil G_s is 2.65, the void ratio e is 1.5, and the inclination angle β of the brittle-fractured soil deposition surface of the shear band is 0°. If the pore space of the shear band will be connected in series to form a tubular outlet, and the efficiency coefficient E of the flow velocity of water in the tubular outlet is only 1%, the calculated particle bottom velocity v_b is 0.088 m/s. Under the above conditions, it is known from Table 1 that the bottom velocity v_b for the brittle-fractured particles with a particle size $D_p \leq 0.5$ mm is greater than the critical bottom velocity v_{bc}; so there is a slight piping failure problem.

When the particles with their sizes $D_p \leq$ 0.5 mm have flowed out, the void ratio e increases from 1.5 to 2.0, and the efficiency coefficient E increases from 1% to 5%, the calculated particle bottom velocity v_b = 0.44 m/s. Under the above conditions, it is known from Table 1 that the bottom velocity v_b for the brittle-fractured particles with a particle size $D_p \leq 1$ cm is greater than the critical bottom velocity v_{bc}; so there is a significant problem of piping failure.

When the particles with their sizes $D_p \leq 1$ cm have flowed out, the void ratio e increases from 2.0 to 2.5 and the efficiency coefficient E increases from 5% to 10%, the calculated particle bottom velocity v_b = 0.88 m/s. Under the above conditions, it is known from Table 1 that the bottom flow velocity v_b for the brittle-fractured particles with a particle size $D_p \leq$ 5 cm is greater than the critical bottom flow velocity v_{bc}; so there is a very significant problem of piping failure.

Identification of Shear Bands Existing in the Area Around Gangweigou Creek Floodway

1) Using the distribution map of epicenters of historical earthquakes

For the vicinity of Gangweigou Creek Floodway, the distribution map of epicenters of historical earthquakes in Taiwan shown in Figure 9 can be used to identify the shear bands. The identification results shown in Figure 9 reveal that there are four groups of shear bands in the area adjacent to Gangweigou Creek Floodway, and their strikes are $N73^{\circ}E$ (white line), $N35^{\circ}E$ (green line), $N20^{\circ}W$ (blue line), and $N60^{\circ}W$ (orange line), respectively.

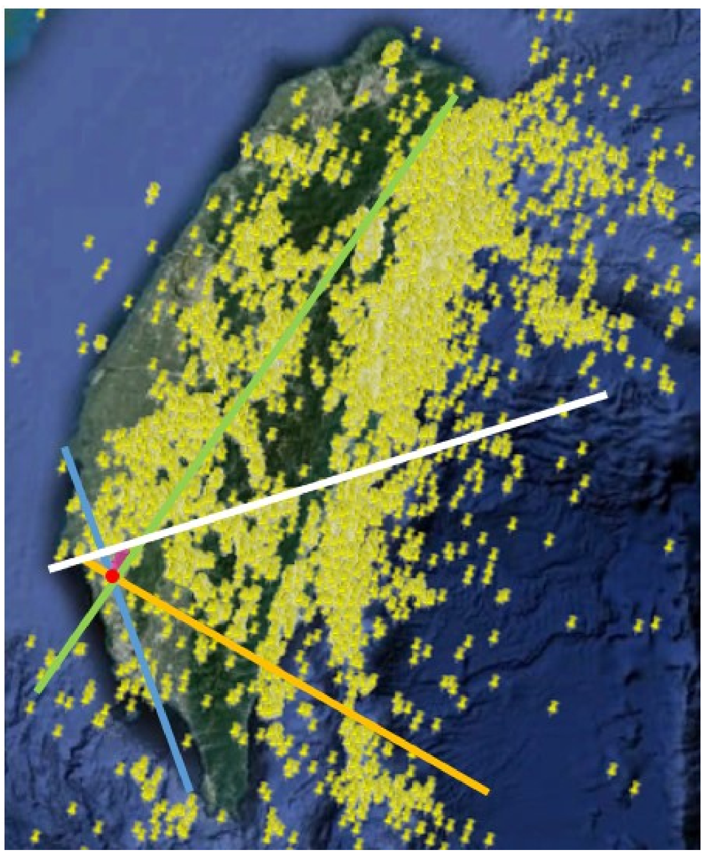

Note: The location of the red dot is the damage location of Gangweigou Creek Floodway

Figure 9. Shear bands identified by using the epicenter distribution map of historical earthquakes in Taiwan (Google Earth, 2020; Central Weather Bureau, 2020).

2) Using satellite image

For the area adjacent to Gangweigou Creek Floodway, the satellite image shown in Figure 10 can be used to identify the shear textures, and the identification results are also shown in Figure 10. There are four shear textures with different strikes in the total shear band width of principal displacement shear D in the area adjacent to Gangweigou Creek Floodway, and the strike of the principal displacement shear D (white line) is $N73^{\circ}E$, the strike of the thrust shear P (pink line) is $N82^{\circ}W$, the strike of the Riedel shear R (green line) is $N35^{\circ}E$, the strike of the conjugate Riedel shear R’ (red line) is $N5^{\circ}W$, and the strike of the compression texture S (blue line) is $N20^{\circ}W$.

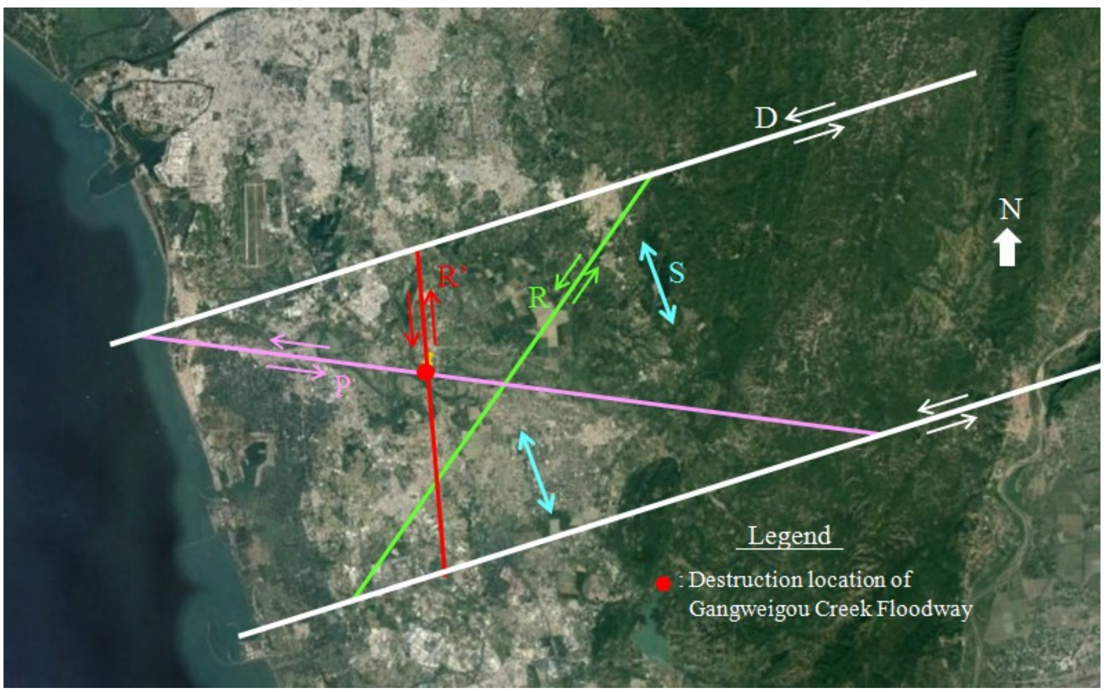

Legend
D: Principal displacement shear
P: Thrust shear
R: Riedel shear
R’: Conjugate Riedel shear
S: Compression texture

Figure 10. Using satellite imagery to identify the shear textures within the total width of a shear band (Background image from Google Earth, 2020).

3) Using GPS velocity vector distribution

For the area adjacent to Gangweigou Creek Floodway, the GPS velocity vector distribution map shown in Figure 11 can be used to identify the shear bands, and the identification results are also shown in Figure 11. There are four shear bands with different strikes in the vicinity of Gangweigou Creek Floodway, and their strikes are $N73^{\circ}E$ (white line) 、 $N35^{\circ}E$ (green line) 、 $N20^{\circ}W$ (blue line) 、 and $N60^{\circ}W$ (orange line), respectively.

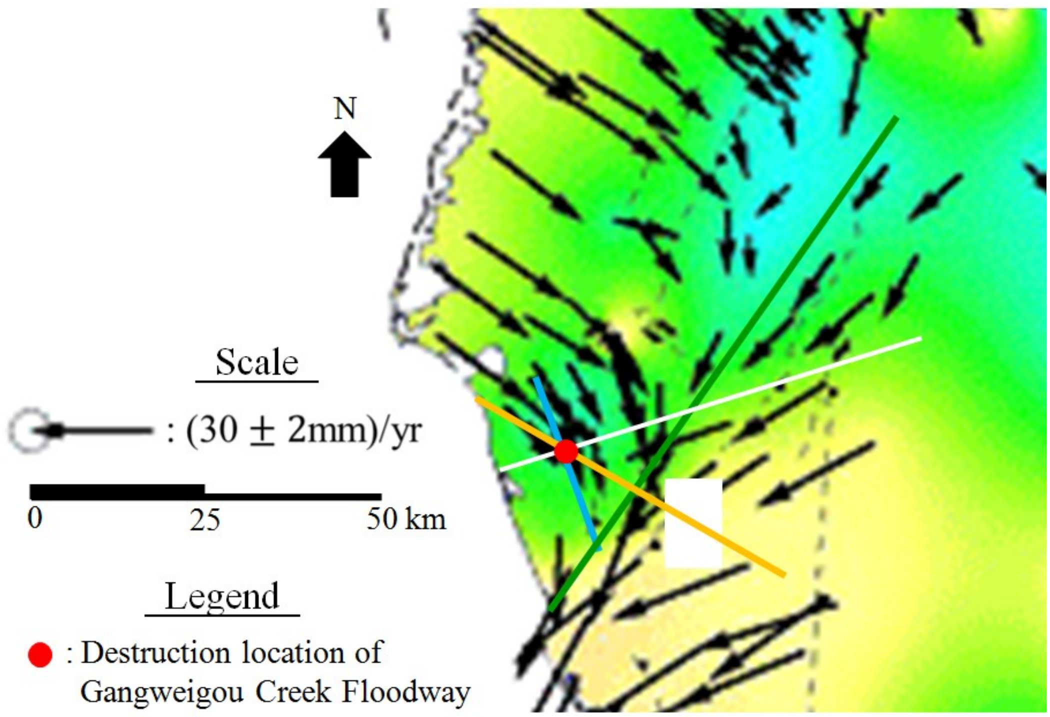

(a) GPS velocity vectors in 2007
(GPSLAB, 2007)

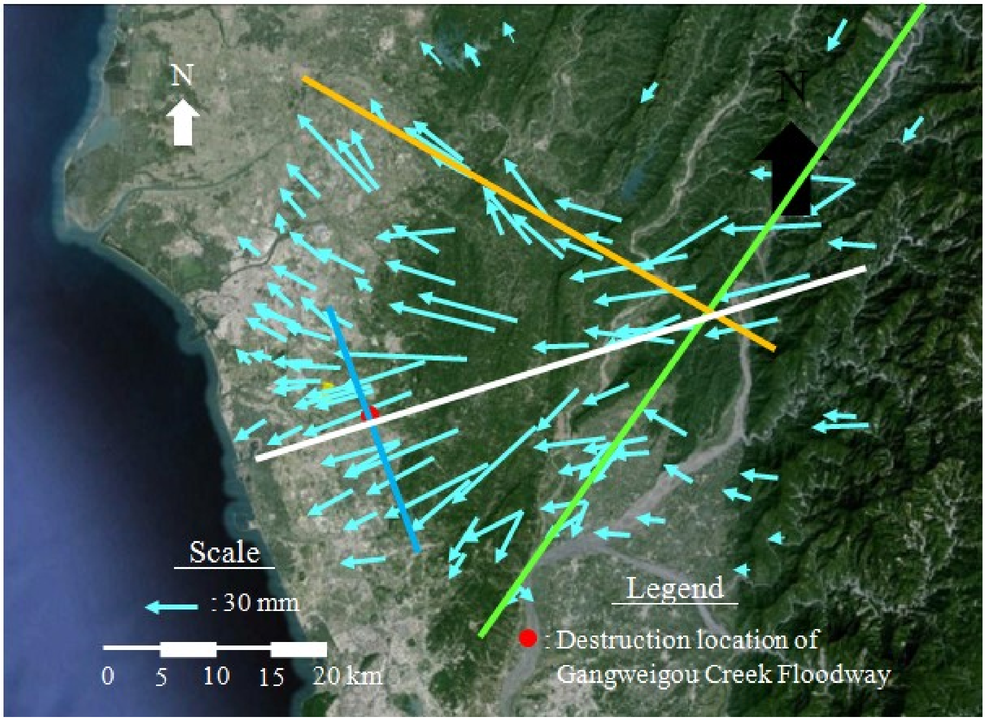

(b) GPS velocity vectors of the 2016 Meinong Earthquake
(Google Earth, 2020; Central Geological Survey, MOEA, 2017)

Figure 11. Using GPS velocity vectors to identify shear bands.

Comparison and Discussion

1) Figures 12a and 12b show the satellite historical image maps before and after the destruction of Gangweigou Creek Floodway, respectively. Figure 12c clearly shows the four piping-induced landslide areas A, B, C, and D on the two sides of Gangweigou Creek Floodway. The piping-induced landslide area A is along the Gangweigou Creek Floodway, and five groups of shear bands or shear textures can be identified and their strikes are $N73^{\circ}E$ (white line), $N5^{\circ}W$ (red line), $N20^{\circ}W$ (blue line), $N60^{\circ}W$ (orange line), and $N82^{\circ}W$ (pink line), respectively; the piping-induced landslide area B is located on the southeast side of the piping-induced landslide area A, two groups of shear bands or shear textures can be identified and their strikes are $N60^{\circ}W$ (orange line) and $N82^{\circ}W$ (pink line), respectively; the piping-induced landslide area C is located in the north of the piping-induced landslide area B, three groups of shear bands or shear textures can be identified and their strikes are $N73^{\circ}E$ (white line), $N20^{\circ}W$ (blue

line), and $N82^{\circ}W$ (pink line), respectively; the piping-induced landslide area D is located in the northwest of the piping-induced landslide area C, three groups of shear bands or shear textures can be identified and their strikes are $N20^{\circ}W$ (blue line), $N60^{\circ}W$ (orange line), and $N82^{\circ}W$ (pink line), respectively.

(a) Before the occurrence of piping failures (2013/11/26)

(b) After the occurrence of piping failures (2015/12/13)

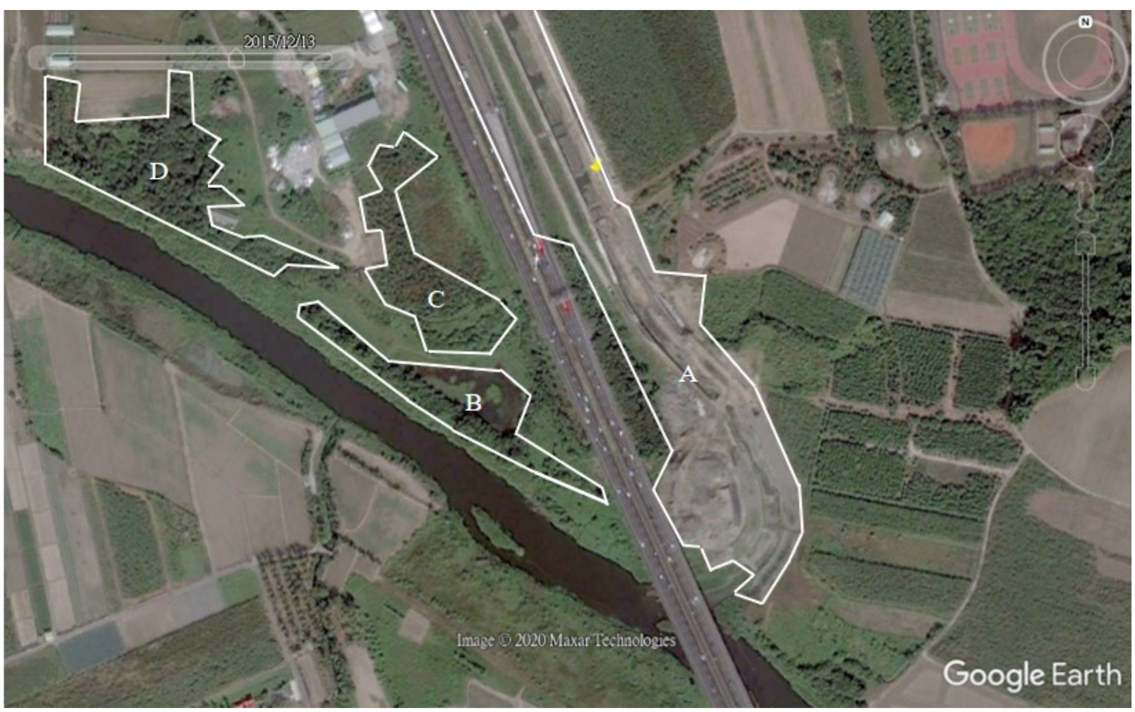

(c) The piping-induced landslide areas A, B, C, and D

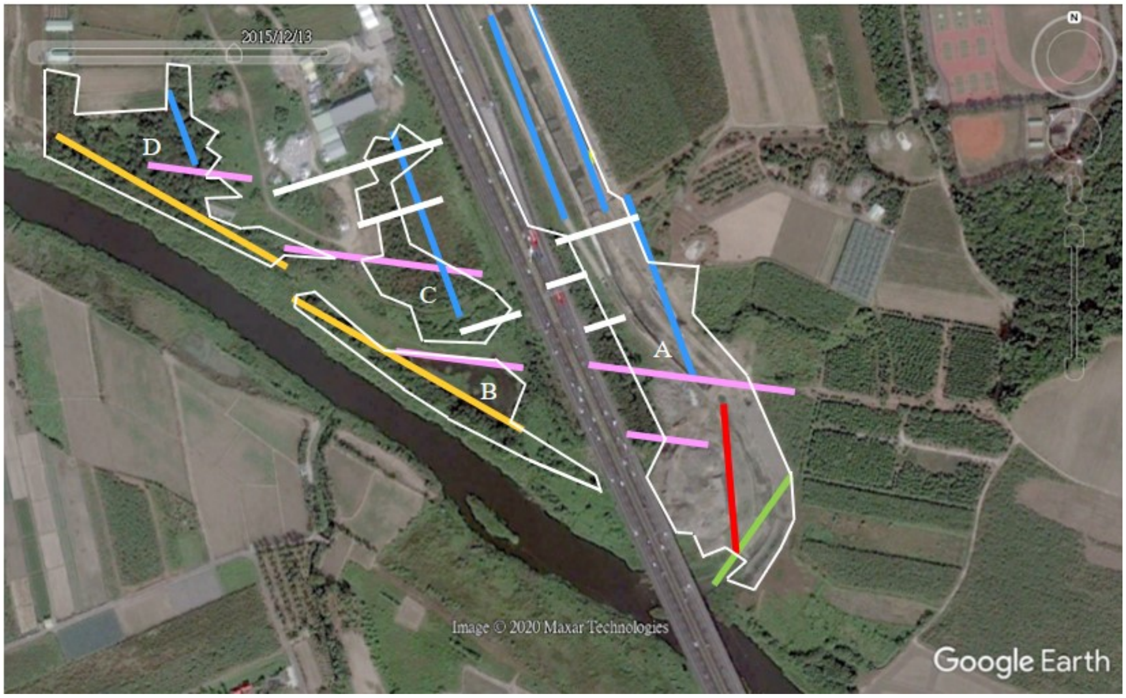

(d) Shear bands or shear textures existing in the areas A, B, C, D

Figure 12. Shear bands or shear textures identified in the piping-induced landslide areas. (Background image from Google Earth, 2020)

2) Under the lateral compression of the soil, when the strain goes deep into the plastic range, localizations of deformations for the soil will be induced due to strain softening, which will lead to a brittle-fractured shear band. The shear banding effect will make the soil particles appear in a highly oriented arrangement, and the shear resistance will be greatly reduced. The mass-conserved steady-state seepage flow will also become a mass-non-conserved unsteady-state pipe flow. Afterwards, groundwater entrains brittle-fractured soil particles and flows out along the pipelines formed in the shear bands.

3) The piping failure model proposed by Terzaghi is based on groundwater seepage flow, which is generally present in the non-shear band area. The piping failure model proposed by the authors is based on groundwater pipe flow, and the pipe flow only exists locally in the shear band. Because the groundwater seepage flow theory is completely incompatible with the groundwater pipe flow theory, Terzaghi use the seepage flow theory to define the piping fail-

ure, which obviously does not meet the actual needs.

4) The total length of Gangweigou Creek Floodway is 3769 m, and the length of local piping failure is only 170 m. During the early stage of piping failure, small particles, such as silt-like and fine-sand-like particles will first flow out, as shown in Figure 13; then the size of the pipeline and the efficiency coefficient of the pipe flow will increase. Larger particles, such as coarse-sand-like or gravel-like particles, may have the chance to flow out. Therefore, the piping failure mechanism proposed by the authors is consistent with the actual phenomenon of piping failure.

Figure 13. The outflow of silt occurred in the early stage of piping failure (Hsu, 2018).

5) For Gangweigou Creek Floodway, the safety factor *FS* of the piping resistance obtained by adopting the formula proposed by Terzaghi is as high as 3.07 (for one-step sheet pile wall) and 3.52 (for two-step sheet pile wall). Under such circumstances, the technician will judge that piping failure will not occur.

6) The case study of piping failure shows that the governing equation for the initiation of piping failure proposed by the authors can help the technician to accurately determine whether piping failure will occur or not.

Conclusions and Suggestions

Conclusions

Floodways often control the flood from entering flood-prone areas by intercepting and straightening, thereby making flood-prone areas reach the design goal of not suffering from flooding. However, the meandering riverbeds entering the flood-prone areas imply shear bands with different strikes. The amount of shear banding will be accumulated in tectonic earthquakes, which will affect the safety of the floodway. Since the current design specifications for hydraulic structures do not fortify the shear banding effect, it is easy for the floodway to locally induce piping failure during the flooding process. In view of this, the authors draw the following five conclusions through the proposed piping failure mechanism and the case study of the Gangweigou Creek Floodway:

1) Using the epicenter distribution map of historical earthquakes, satellite image map, GPS velocity vector distribution map, and on-site image map, it can be identified that the existing shear bands with various strikes such as $N73^{\circ}E$, $N35^{\circ}E$, $N5^{\circ}W$, $N20^{\circ}W$, $N60^{\circ}W$, and $N82^{\circ}W$ are located in the areas adjacent to Gangweigou Creek Floodway.

2) In the design, the area where the floodway passes should be divided into non-shear band area and shear band area; the groundwater flow pattern in non-shear band area is steady-state seepage flow with conserved mass, while the groundwater flow pattern in shear band area is a unsteady-state pipe flow with non-conserved mass.

3) The more significant the shear banding effect, the higher the degree of orientation of the particles; the higher the degree of orientation of the particles, the closer the groundwater flow pattern to the pipe flow; the larger the size of pipeline, the larger the energy efficiency of the pipe flow. Under the above conditions, the piping failure is more likely to occur.

4) The piping failure mechanism and the safety factor of piping failure resistance *FS* proposed by Terzaghi are based on groundwater seepage flow. For the localized piping failure in the shear band, the case study results show that the Terzaghi's mechanism and safety factor will not give analysis results consistent with the facts.

5) The piping failure mechanism and the governing equation for the initiation of piping flow proposed by the authors are based on groundwater pipe flow. For the localized piping failure in the shear band, the case study results show that the authors' mechanism and governing equation will give analysis results consistent with the facts.

Suggestions

Since the formation of deep grooves in the riverbed is caused by shear banding effect, the authors make the following two suggestions based on the above five conclusions:

1) Design specifications for hydraulic structures, in addition to the existing regulations, are suggested to include shear banding effect. Thereafter, it is stipulated that all shear bands existing in the site are to be identified in the planning stage, and then the degree of orientation and engineering properties of the brittle-fractured particles in the shear band are be investigated or tested, so as to ensure that the design results provided by the technicians are safe.
2) During the occurrence of piping failure, brittle-fractured particles, such as silt-like, sand-like, and gravel-like particles, will flow out in order from small particle size to large particle size. Therefore, it is suggested to include the piping failure mechanism and the governing equation for the initiation of the piping failure proposed by the authors' in the specification, so as to obtain analysis results that are consistent with the facts.

References

Central Geological Survey, MOEA. Integrated Geological Data Inquiry System, Website: http://www.moeacgs.gov.tw/app/index.jsp, 2017.

Central Weather Bureau, Ministry of Transportation and Communications. Disastrous earthquakes, Website: http://www.cwb.gov.tw/V7/earthquake/damage_eq.htm, 2020.

epaper.wra.gov.tw, "Reconstruction Project of the Middle Reaches of Gangweigou Creek Floodway: To Ensure the Effectiveness of Flood Control," Sixth River Management Office, Water Resources Agency, Ministry of Economic Affairs, 2015.

Google Earth, Website: http://www.google.com.tw/intl/zh-TW/earth/, 2020.

GPS LAB, Website: http://gps.earth.sinica.edu.tw/, 2007.

Hsu, T.-S., **The Major Cause of Earthquake Disasters: Shear Banding**, Institute of Mitigation for Earthquake Shear Banding Disasters, p. 235, 2018.

Hsu , T.-S., Chiu, S.-E., Hsu, S., Ho, C.-C., "A Particle Floating Model for the Initiation of Debris Flows," **37th National Conference on Theoretical and Applied Mechanics & The 1st International Conference on Mechanics, Procedia Engineering**, Elsevier, Vol. 79, pp. 606-611, 2014.

Qi, S.-Y., "Gangweigou Creek Floodway," HouseFun News, Website: https://news.housefun.com.tw/news/article/13417458737.html, 2014.

Terzaghi, K., **Theoretical Soil Mechanics**, John Wiley & Sons, Inc., pp. 257-262, 1943.

Water Resources Bureau of Ministry of Economic Affairs, "Water Conservancy Construction Inspection and Safety Assessment Methods", 2003.

Water Resources Bureau of Ministry of Economic Affairs, "Water Conservancy Construction Inspection and Safety Assessment Technical Specification", 2008.

Wu, J.-F., "The collapse of Gangweigou Creek Floodway," Liberty Times Net, Website: https://news.ltn.com.tw/news/life/breakingnews/1836670, 2016.